

Electronic Supplementary Information

Dynamics of the copper(I)-alkyne interaction and its use in a heteroleptic four-component catalytic rotor

Suchismita Saha,^a Sohom Kundu,^a Pronay Kumar Biswas,^a Michael Bolte,^b Michael Schmittel^{*,a}

^a Center of Micro and Nanochemistry and (Bio)Technology, Organische Chemie I, Universität Siegen, Adolf-Reichwein-Str. 2, D-57068 Siegen, Germany; ^b Institut für Organische Chemie und Chemische Biologie, Johann Wolfgang Goethe-Universität, Max-von-Laue Strasse 7, D-60438 Frankfurt am Main, Germany.

Table of contents

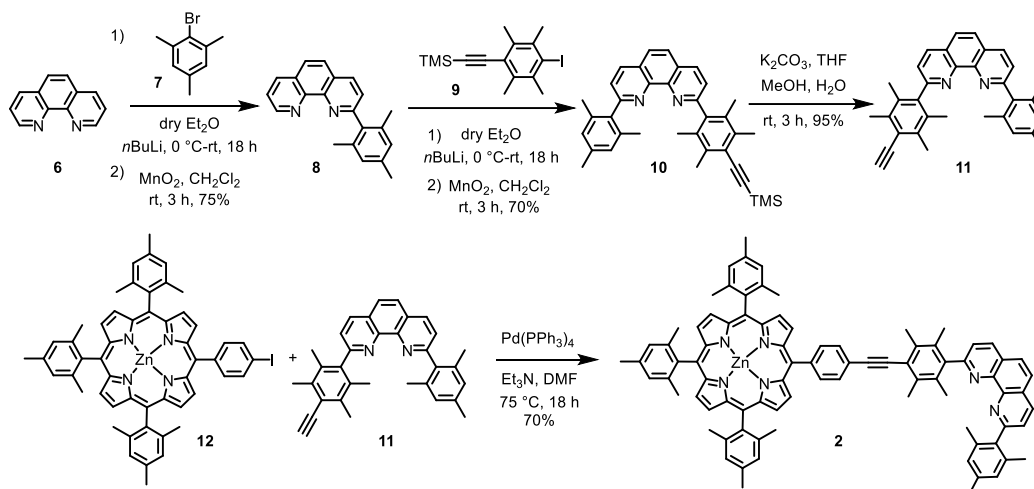
1. Synthesis	S2-S11
1.1 General information	S2
1.2 Synthesis and characterization of ligands	S3-S6
1.3 Synthesis and characterization of complexes	S7-S11
2. NMR spectra: ¹ H, ¹³ C, ¹ H- ¹ H COSY	S13-S23
3. Variable temperature ¹ H NMR spectra	S24
4. DOSY NMR spectra	S25-S26
5. ESI-MS spectra	S27-S28
6. Binding constant determination	S29-S30
7. X-ray crystallography	S31-S34
8. References	S35

1. Synthesis

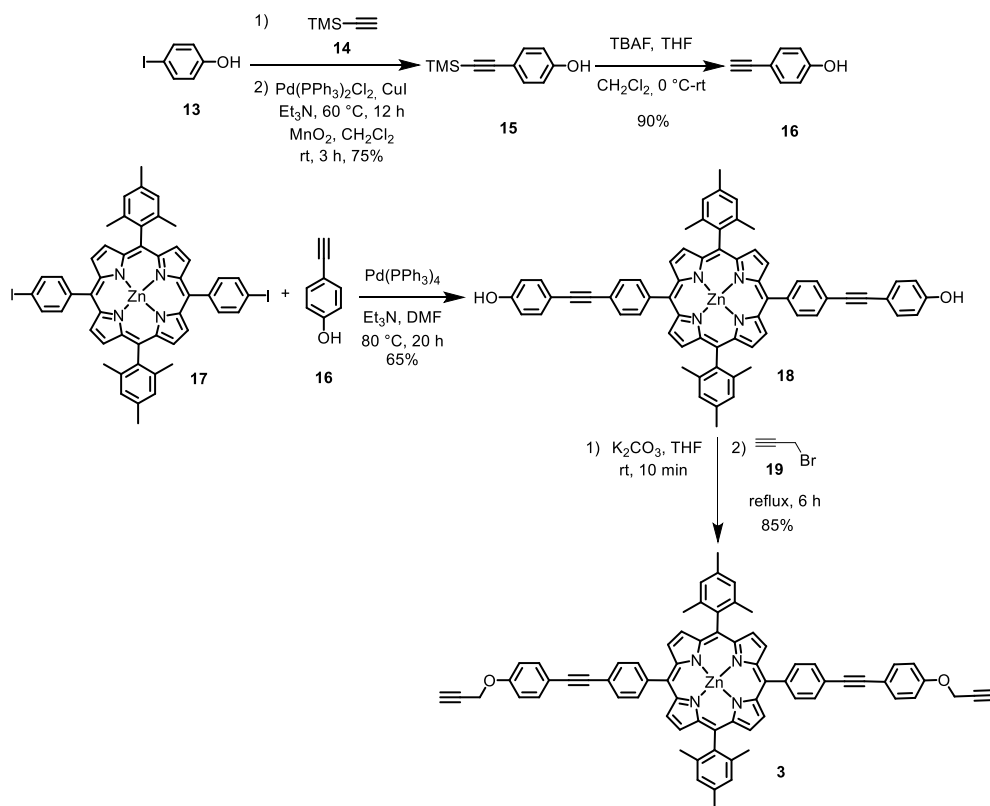
1.1 General information

All solvents were dried by distillation prior to use while commercial reagents were used without any further purification. Bruker Avance (400 MHz), Jeol ECZ 500 (500 MHz) and Varian VNMR-S 600 (600 MHz) spectrometers were used to measure ^1H and ^{13}C NMR spectra applying the deuterated solvent as the lock and residual protiated solvent as internal reference (CDCl_3 : δ_H 7.26 ppm, δ_C 77.0 ppm; CD_2Cl_2 : δ_H 5.32 ppm, δ_C 53.8 ppm, $\text{DMSO}-d_6$: δ_H 2.50 ppm, δ_C 39.52 ppm). The following abbreviations were used to define NMR peak patterns: s = singlet, d = doublet, t = triplet, dd = doublet of doublets, bs = broad signal, m = multiplet. The coupling constant values are given in Hertz (Hz) and, wherever possible, assignments of protons are provided. The numbering of different carbons in different molecular skeletons does not necessarily follow the IUPAC nomenclature rules; it is exclusively provided for assigning NMR signals. All electrospray ionization (ESI-MS) spectra were recorded on a Thermo-Quest LCQ deca and the theoretical isotopic distributions of the mass signals were calculated (<https://omics.pnl.gov/software/molecular-weight-calculator>) using a molecular weight calculator software. Melting points of compounds were measured on a BÜCHI 510 instrument and are not corrected. Infrared spectra were recorded on a Perkin Elmer Spectrum-Two FT-IR spectrometer. Elemental analysis was performed using the EA-3000 CHNS analyzer. UV-vis spectra were recorded on a Varian Cary 100 BioUV/Vis spectrometer. Column chromatography was performed either on silica gel (60-400 mesh) or neutral alumina (Fluka, 0.05-0.15 mm, Brockmann Activity 1). Merck silica gel (60 F254) or neutral alumina (150 F254) sheets were used for thin layer chromatography (TLC). All complexations were performed directly in the NMR tube using CD_2Cl_2 as solvent.

1.2 Synthesis and characterization of ligands



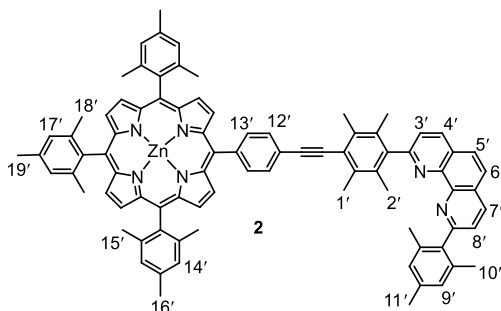
Scheme S1. Reaction scheme to synthesis stator **2**. Synthesis of **8**,¹ **9**,² **10**,² **11**² and **12**³ was done following literature-known procedures.



Scheme S2. Reaction scheme to synthesis rotator **3**. Synthesis of **15**,⁴ **16**⁴ and **17**³ was done following literature-known procedures.

Synthesis of stator **1**⁵ and model compounds **4**⁶ and **5**⁷ was accomplished by a literature-known procedure.

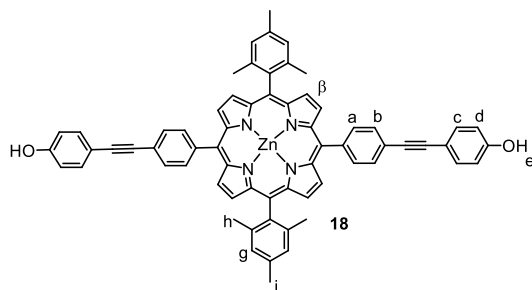
Synthesis of **2**⁸



Under N₂ atmosphere, compounds **12** (100 mg, 107 μmol) and **11** (195 mg, 430 μmol) were dissolved in dry DMF (20 mL) and dry Et₃N (20 mL) in a sealed tube. The mixture was degassed by two freeze-pump-thaw cycles. Then, Pd(PPh₃)₄ (15.0 mg, 13.0 μmol) was added under N₂ atmosphere. After degassing again by freeze-pump-thaw cycles, the reaction mixture was stirred at 75 °C for 18 h. The solvent was evaporated under reduced pressure and the residue worked up with ice-cold water to remove DMF. The organic part was extracted with CH₂Cl₂, dried over anhydrous Na₂SO₄ and concentrated. The compound was first purified by column chromatography (SiO₂) using CH₂Cl₂ in as eluent (*R*_f = 0.3). It was finally purified by size exclusion chromatography using SX-3 biobead using THF as eluent to afford a violet solid (94.5 mg, 70%).

mp: > 250 °C. **¹H NMR (CD₂Cl₂, 400 MHz):** δ = 1.84 (s, 12H, 15'-H), 1.85 (s, 6H, 18'-H), 2.01 (s, 6H, 1'-H), 2.07 (s, 6H, 10'-H), 2.36 (s, 3H, 11'-H), 2.61 (s, 3H, 19'-H), 2.62 (s, 6H, 16'-H), 2.69 (s, 6H, 2'-H), 6.98 (s, 2H, 9'-H), 7.29 (s, 2H, 17'-H), 7.30 (s, 4H, 14'-H), 7.59 (d, ³*J* = 8.2 Hz, 1H, 3'/8'-H), 7.60 (d, ³*J* = 8.2 Hz, 1H, 8'/3'-H), 7.93 (s, 2H, 5'+6'-H), 7.98 (d, ³*J* = 8.4 Hz, 2H, 12'-H), 8.25 (d, ³*J* = 8.4 Hz, 2H, 13'-H), 8.36 (d, ³*J* = 8.2 Hz, 1H, 4'/7'-H), 8.39 (d, ³*J* = 8.2 Hz, 1H, 7'/4'-H), 8.70 (s, 4H, β-H), 8.76 (d, ³*J* = 4.6 Hz, 2H, β-H), 8.93 (d, ³*J* = 4.6 Hz, 2H, β-H) ppm.

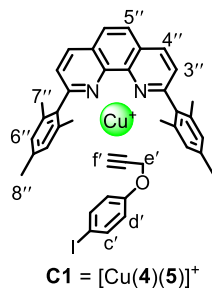
Synthesis of **18**⁹



In a dry sealed tube, compounds **17** (250 mg, 247 μmol) and **16** (233 mg, 1.98 mmol) were taken and dissolved in 20 mL of DMF and 20 mL of triethylamine. The solution was deaerated by the freeze-pump-thaw method twice. To this mixture, $\text{Pd}(\text{PPh}_3)_4$ (57.0 mg, 49.4 μmol) was added. The solution was once more deaerated using the freeze-pump-thaw method and it was allowed to stir at 80 $^\circ\text{C}$ for 20 h. All the solvents were then evaporated under vacuum. The residue was worked up using CH_2Cl_2 and ice-cold water. The organic part was separated, dried over Na_2SO_4 and filtered to get rid of solids. The filtrate was evaporated under vacuum and subjected to column chromatography on silica (SiO_2) using 50% ethyl acetate in hexane ($R_f = 0.4$). Finally, the compound was purified over SX-3 bio-bead using THF as eluent to obtain the violet compound (159 mg, 65%). **Mp**: > 250 $^\circ\text{C}$. **^1H NMR (CDCl_3 , 500 MHz)**: $\delta = 1.83$ (s, 12H, h-H), 2.63 (s, 6H, i-H), 5.00 (s, 2H, e-H), 6.89 (d, $^3J = 8.4$ Hz, 4H, d-H), 7.29 (s, 4H, g-H), 7.58 (d, $^3J = 8.4$ Hz, 4H, c-H), 7.89 (d, $^3J = 8.4$ Hz, 4H, b-H), 8.22 (d, $^3J = 8.4$ Hz, 4H, a-H), 8.79 (d, $^3J = 4.4$ Hz, 4H, β -H), 8.90 (d, $^3J = 4.4$ Hz, 4H, β -H) ppm.

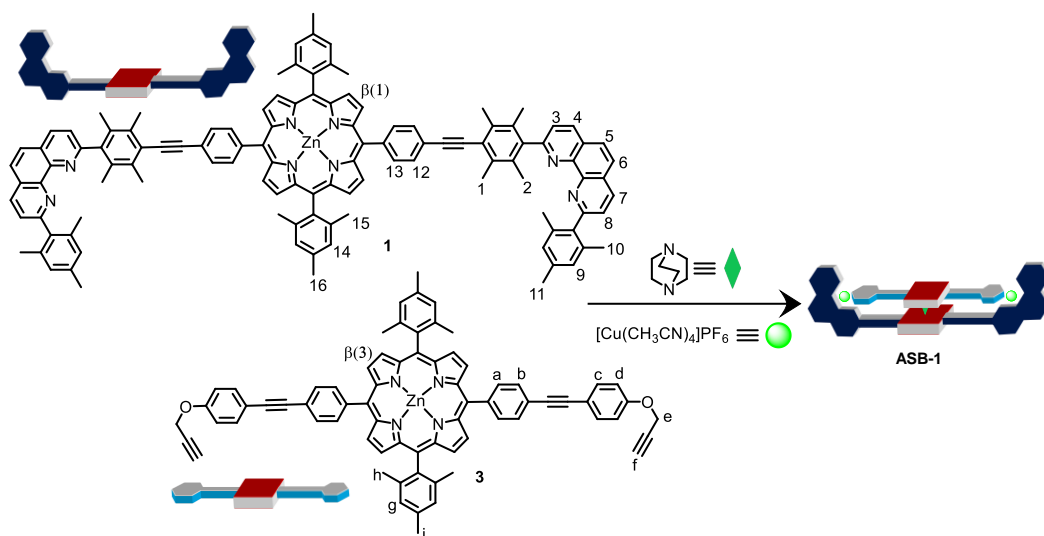
1.3 Synthesis and characterization of complexes

Synthesis of model complex **C1**



In an NMR tube, compound **4** (565 μg , 1.36 μmol), [Cu(CH₃CN)₄]PF₆ (506 μg , 1.36 μmol) and **5** (350 μg , 1.36 μmol) were dissolved in 550 μL of CD₂Cl₂ to quantitatively furnish complex **C1** = [Cu(4)(5)]⁺. **IR (KBr):** ν = 507, 559, 625, 733, 838, 1017, 1084, 1144, 1177, 1221, 1285, 1401, 1484, 1510, 1586, 1611, 1970, 2855, 2918, 2969, 3189, 3238 cm⁻¹. **¹H NMR (CD₂Cl₂, 400 MHz):** δ = 2.05 (s, 12H, 7''-H), 2.34 (s, 6H, 8''-H), 2.68 (t, ³J = 2.2 Hz, 1H, f'-H), 4.09 (d, ³J = 2.2 Hz, 2H, e'-H), 6.60 (d, ³J = 9.0 Hz, 2H, d'-H), 7.03 (s, 4H, 6''-H), 7.58 (d, ³J = 9.0 Hz, 2H, c'-H), 7.92 (d, ³J = 8.2 Hz, 2H, 3''-H), 8.20 (s, 2H, 5''-H), 8.74 (d, ³J = 8.2 Hz, 2H, 4''-H) ppm. **ESI-MS:** m/z (%) 738.4 (100) [Cu(4)(5)]⁺.

Synthesis of **ASB-1**

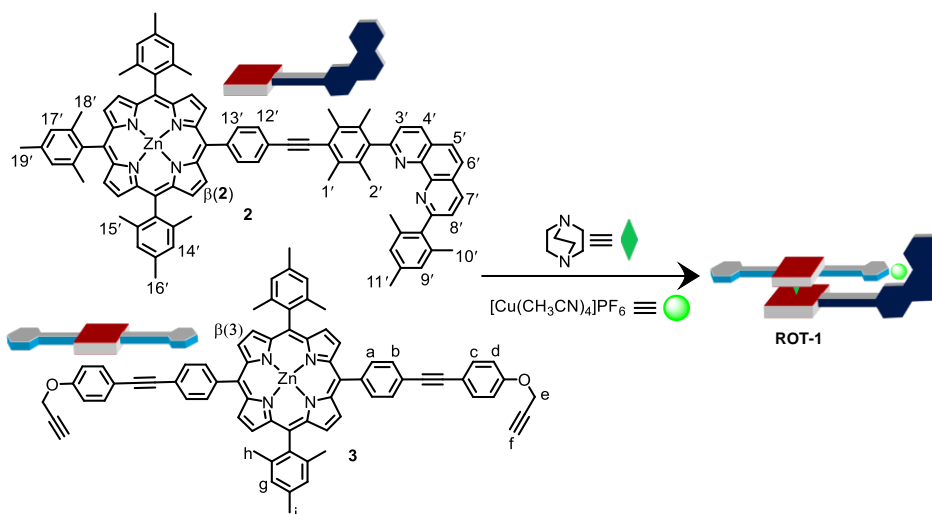


All the spacer protons 12-H, 13-H, a-H and b-H are assigned as s-H. After complexation 14-H, 15-H, g-H and h-H split into 1:1 ratio and they are assigned as 14'-H, 14'-H, 15'-H, 15'-H, g'-H, g'-H, h-H and h'-H, respectively. We see a loss of symmetry in the ^1H NMR due to the restricted rotation of the phenyl group in **ASB1**.

In an NMR tube, compound **1** (1.15 mg, 690 nmol), rotator **3** (738 μg , 690 nmol), DABCO (77.4 μg , 690 nmol) and $[\text{Cu}(\text{CH}_3\text{CN})_4]\text{PF}_6$ (514 μg , 1.38 μmol) were dissolved in 550 μL of CD_2Cl_2 to furnish the complex **ASB-1** in quantitative yield. **mp**: > 250 $^\circ\text{C}$. **IR (KBr)**: $\nu = 560, 641, 727, 797, 809, 846, 972, 996, 1064, 1081, 1103, 1179, 1204, 1226, 1286, 1306, 1337, 1378, 1458, 1492, 1511, 1551, 1587, 1608, 1694, 2213, 2729, 2842, 2870, 2916, 2956 \text{ cm}^{-1}$. **^1H NMR (CD_2Cl_2 , 400 MHz)**: $\delta = -4.57 - -4.53$ (m, 6H, DABCO-H), $-4.49 - -4.45$ (m, 6H, DABCO-H), 1.11 (s, 6H, h/15-H), 1.13 (s, 6H, 15/h-H), 1.67 (s, 6H, h'/15'-H), 1.77 (s, 6H, 15'/h'-H), 2.02 (s, 12H, 1-H), 2.18 (s, 12H, 10-H), 2.47 (s, 6H, 11-H), 2.58 (s, 6H, 16-H), 2.59 (s, 6H, i-H), 2.64 (s, 12H, 2-H), 3.10 (t, $^3J = 1.4 \text{ Hz}$, 2H, f-H), 3.60 (d, $^3J = 1.4 \text{ Hz}$, 4H, e-H), 6.77 (d, $^3J = 8.8 \text{ Hz}$, 4H, d-H), 7.07 (s, 2H, g/14-H), 7.08 (s, 2H, 14/g-H), 7.10 (d, $^3J = 8.0 \text{ Hz}$, 2H, s-H), 7.21 (s, 4H, 9-H), 7.31 (d, $^3J = 8.0 \text{ Hz}$, 2H, s-H), 7.33 (s, 2H, g'/14'-H), 7.34 (s, 2H, 14'/g'-H), 7.75 (d, $^3J = 8.8$

Hz, 4H, c-H), 7.84 (d, $^3J = 8.0$ Hz, 2H, s-H), 7.85 (d, $^3J = 8.2$ Hz, 2H, 8/3-H), 7.90 (d, $^3J = 8.0$ Hz, 2H, s-H), 7.93-7.99 (m, 4H, s-H), 8.02 (d, $^3J = 8.2$ Hz, 2H, 3/8-H), 8.07 (d, $^3J = 8.0$ Hz, 2H, s-H), 8.21 (bs, 2H, s-H), 8.29 (d, $^3J = 8.8$ Hz, 2H, 6/5-H), 8.32 (d, $^3J = 8.8$ Hz, 2H, 5/6-H), 8.35 (d, $^3J = 4.6$ Hz, 4H, $\beta(1)$ -H), 8.36 (d, $^3J = 4.6$ Hz, 4H, $\beta(3)$ -H), 8.54 (d, $^3J = 4.6$ Hz, 4H, $\beta(1)$ -H), 8.59 (d, $^3J = 4.6$ Hz, 4H, $\beta(3)$ -H), 8.83 (d, $^3J = 8.2$ Hz, 2H, 7/4-H), 8.89 (d, $^3J = 8.2$ Hz, 2H, 4/7-H) ppm. **ESI-MS:** m/z (%) 1489.1 (100) $[\text{Cu}_2(\mathbf{1})(\mathbf{3})(\text{DABCO})]^{2+}$. **Elemental analysis:** Anal. Calcd for $\text{C}_{194}\text{H}_{160}\text{N}_{14}\text{O}_2\text{Zn}_2\text{Cu}_2\text{P}_2\text{F}_{12} \cdot 5\text{CH}_2\text{Cl}_2 \cdot 2\text{CH}_3\text{CN}$: C, 64.61; H, 4.70; N, 5.94. Found: C, 64.64; H, 4.91; N, 6.10.

Synthesis of **ROT-1**

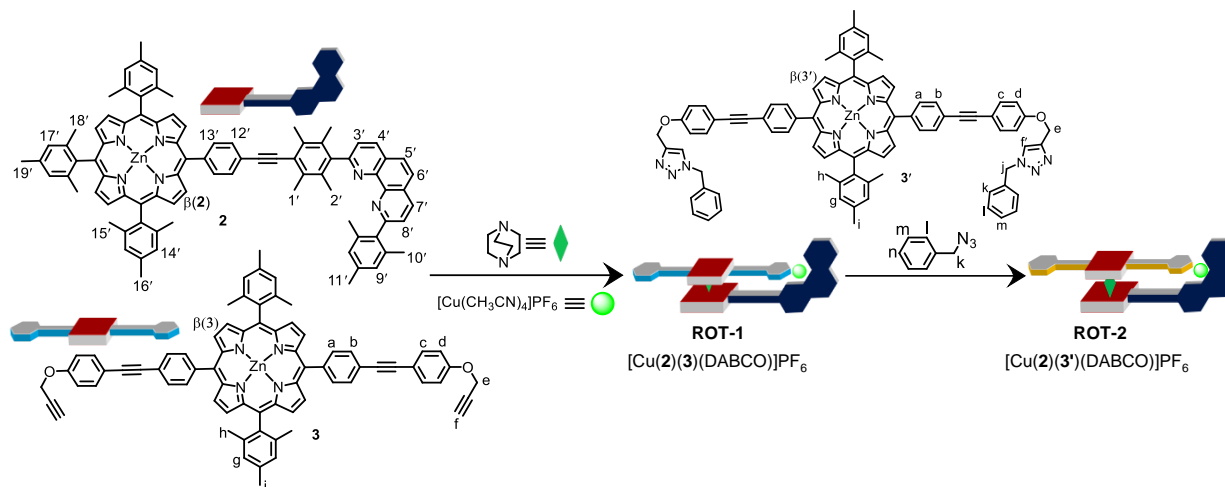


All the spacer protons 12'-H, 13'-H, a-H and b-H are assigned as s-H.

In an NMR tube, compound **2** (976 μg , 776 nmol), rotator **3** (831 μg , 776 nmol), DABCO (87.1 μg , 776 nmol) and $[\text{Cu}(\text{CH}_3\text{CN})_4]\text{PF}_6$ (289 μg , 776 nmol) were dissolved in 550 μL of CD_2Cl_2 to furnish the complex **ROT-1** in quantitative yield. **mp:** > 250 $^\circ\text{C}$. **IR (KBr):** $\nu = 640, 668, 722, 798, 809, 831, 851, 996, 1062, 1103, 1139, 1175, 1204, 1225, 1286, 1304, 1336, 1378, 1400,$

1456, 1479, 1511, 1608, 1696, 1809, 2213, 2730, 2868, 2917, 2954, 3116, 3307 cm^{-1} . **^1H NMR** (CD_2Cl_2 , **600 MHz**): $\delta = -4.51$ (bs, 6H, DABCO-H), -4.40 (bs, 6H, DABCO-H), 1.20 (bs, 12H, h-H), 1.47 (bs, 18H, $15'\text{-H}+18'\text{-H}$), 2.03 (s, 6H, $1'\text{-H}$), 2.16 (s, 6H, $10'\text{-H}$), 2.46 (s, 3H, $11'\text{-H}$), 2.58 (s, 9H, $16'\text{-H}+19'\text{-H}$), 2.60 (s, 6H, i-H), 2.65 (s, 6H, $2'\text{-H}$), 2.88 (bs, 2H, f-H), 4.19 (bs, 4H, e-H), 6.93 (d, $^3J = 8.0$ Hz, 4H, d-H), 6.98 (bs, 1H, s-H), 7.15 (d, $^3J = 8.4$ Hz, 1H, s-H), $7.19\text{-}7.34$ (m, 12H, g-H+ $14'\text{-H}+17'\text{-H}+9\text{-H}$), 7.63 (d, $^3J = 8.4$ Hz, 1H, s-H), 7.66 (d, $^3J = 8.4$ Hz, 1H, s-H), 7.72 (d, $^3J = 8.0$ Hz, 4H, c-H), $7.84\text{-}7.90$ (m, 5H, $8'/3'\text{-H}+s\text{-H}$), $7.94\text{-}7.97$ (m, 2H, s-H), 8.00 (d, $^3J = 8.4$ Hz, 1H, $3'/8'\text{-H}$), $8.27\text{-}8.28$ (bs, 2H, s-H), 8.28 (d, $^3J = 8.8$ Hz, 2H, $6'/5'\text{-H}$), 8.31 (d, $^3J = 8.8$ Hz, 2H, $5'/6'\text{-H}$), $8.33\text{-}8.37$ (m, 8H, $\beta(2)\text{-H}+\beta(3)\text{-H}$), $8.53\text{-}8.55$ (m, 8H, $\beta(2)\text{-H}+\beta(3)\text{-H}$), 8.84 (d, $^3J = 8.0$ Hz, 1H, $7'/4'\text{-H}$), 8.88 (d, $^3J = 8.4$ Hz, 1H, $4'/7'\text{-H}$) ppm. **ESI-MS:** m/z (%) 2388.8 (100) $[\text{Cu}(2)(3)]^+$. **Elemental analysis:** Anal. Calcd for $\text{C}_{164}\text{H}_{138}\text{N}_{12}\text{O}_2\text{Zn}_2\text{CuPF}_6\cdot\text{CH}_2\text{Cl}_2$: C, 72.51; H, 5.16; N, 6.15. Found: C, 72.19; H, 4.97; N, 6.48.

Synthesis of ROT-2



All the spacer protons 12'-H, 13'-H, a-H and b-H are assigned as s-H.

In an NMR tube, compound **2** (946 μg , 753 nmol), rotator **3** (806 μg , 753 nmol), DABCO (84.5 μg , 753 nmol) and $[\text{Cu}(\text{CH}_3\text{CN})_4]\text{PF}_6$ (281 μg , 753 nmol) were dissolved in 100 μL of CD_2Cl_2 to furnish the complex **ROT-1** in quantitative yield. Now, benzyl azide (200 μg , 1.50 μmol) and 1 μL of Et_3N were added. Further 300 μL of CD_2Cl_2 was added. The NMR tube was tightly closed and heated at 40 $^\circ\text{C}$ for 24 h. Then all the solvent was evaporated to remove residual Et_3N . The residue was redissolved in 550 μL of CD_2Cl_2 to furnish **ROT-2** in quantitative yield. **mp**: > 250 $^\circ\text{C}$. **^1H NMR (CD_2Cl_2 , 400 MHz)**: $\delta = -4.39$ (bs, 12H, DABCO-H), 1.26 (bs, 12H, h-H), 1.47 (bs, 18H, 15'-H+18'-H), 2.03 (s, 6H, 1'-H), 2.08 (s, 6H, 10'-H), 2.15 (s, 3H, 11'-H), 2.58 (s, 15H, 16'-H+19'+2'-H), 2.59 (s, 6H, i-H), 4.81 (bs, 4H, e-H), 5.52 (s, 4H, j-H), 6.61 (bs, 2H, 9'-H), 6.78 (bs, 4H, d-H), 7.21 (bs, 12H, g-H+14'-H+17'-H+s-H), 7.28-7.30 (m, 6H, k-H+s-H), 7.41-7.48 (m, 8H, l-H+m-H+s-H), 7.61 (d, $^3J = 8.0$ Hz, 4H, c-H), 7.85 (d, $^3J = 7.8$ Hz, 4H, s-H), 7.92-7.94 (m, 4H, 3'-H+8'-H+s-H), 8.21 (s, 2H, 5'-H+6'-H), 8.28 (bs, 2H, $\beta(\mathbf{2})$ -H), 8.30 (bs, 2H, $\beta(\mathbf{2})$ -H), 8.35-8.36 (m, 6H, $\beta(\mathbf{2})$ -H+ $\beta(\mathbf{3}')$ -H), 8.53-8.54 (m, 6H, $\beta(\mathbf{2})$ -H+ $\beta(\mathbf{3}')$ -H), 8.73 (d, $^3J = 8.0$ Hz, 2H,

4'-H+7'-H) ppm. **ESI-MS:** m/z (%) 2655.9 (100) [Cu(2)(3')]⁺. **Elemental analysis:** Anal. Calcd for C₁₇₈H₁₅₂N₁₈O₂Zn₂CuPF₆•5CH₂Cl₂: C, 65.82; H, 4.89; N, 7.55. Found: C, 65.55; H, 4.64; N, 7.32.

2. NMR spectra: ^1H , ^{13}C , ^1H - ^1H COSY

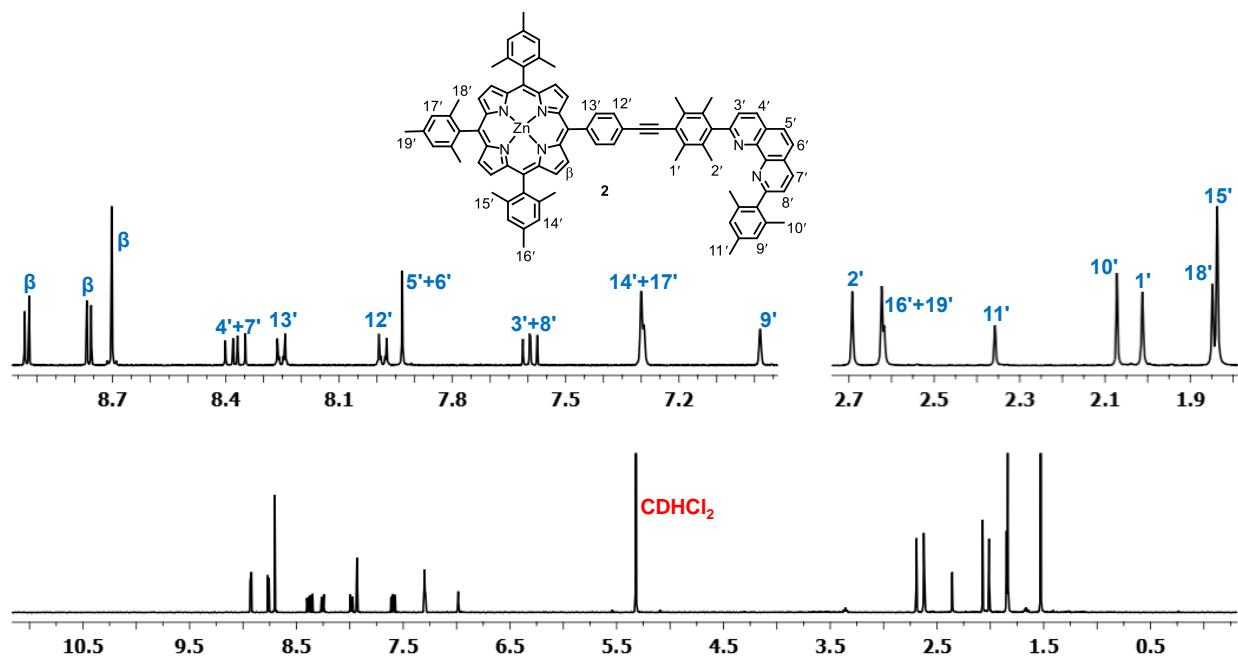


Figure S1. ^1H NMR of compound **2** in CD_2Cl_2 (400 MHz, 298 K).

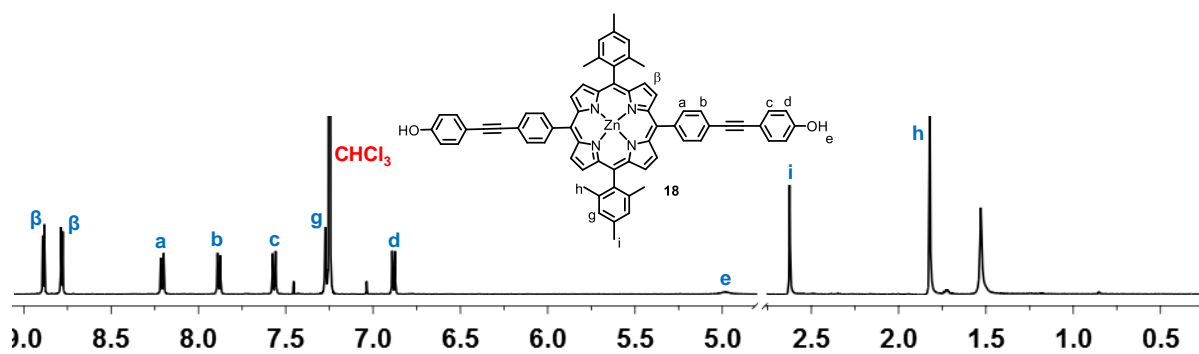


Figure S2. ^1H NMR of compound **18** in CDCl_3 (500 MHz, 298 K).

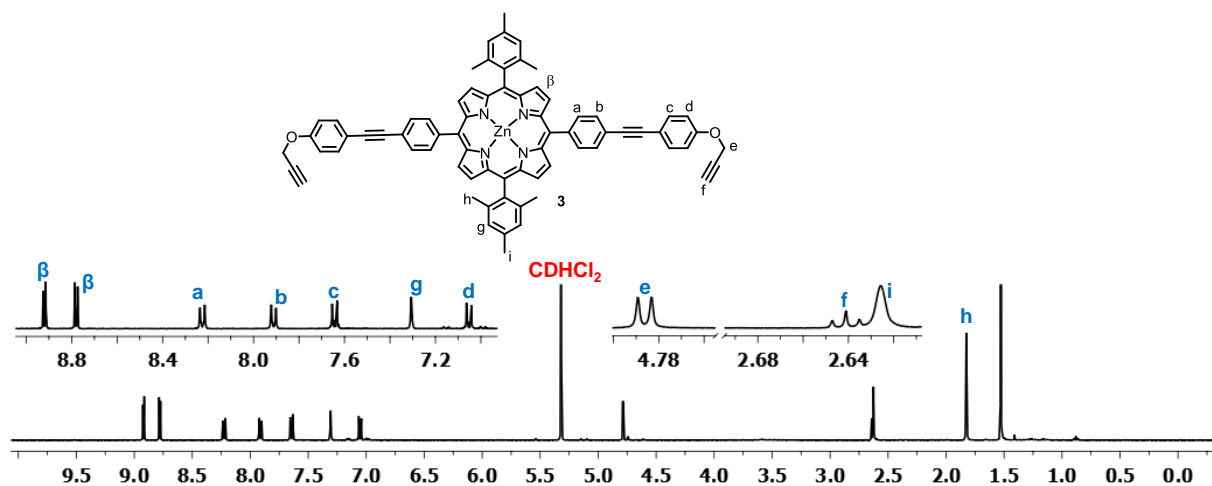


Figure S3. ^1H NMR of compound **3** in CD_2Cl_2 (400 MHz, 298 K).

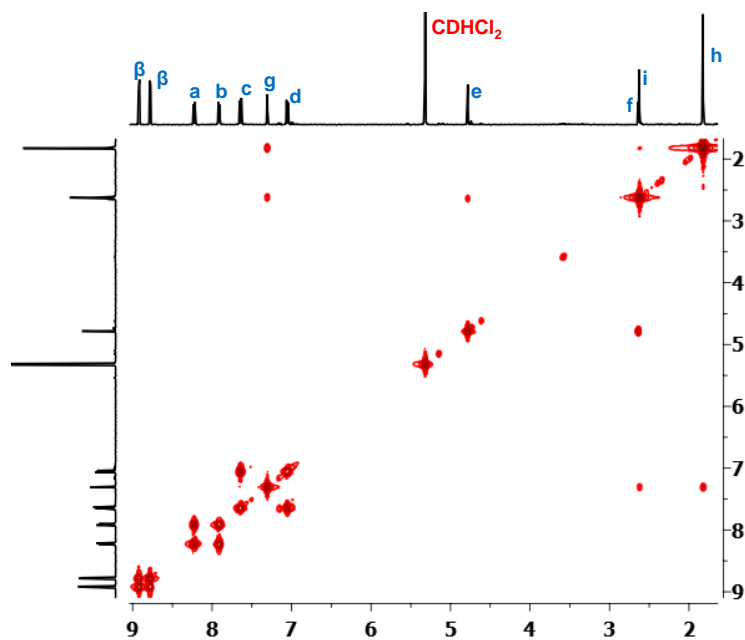


Figure S4. ^1H - ^1H COSY NMR of compound **3** in CD_2Cl_2 (400 MHz, 298 K).

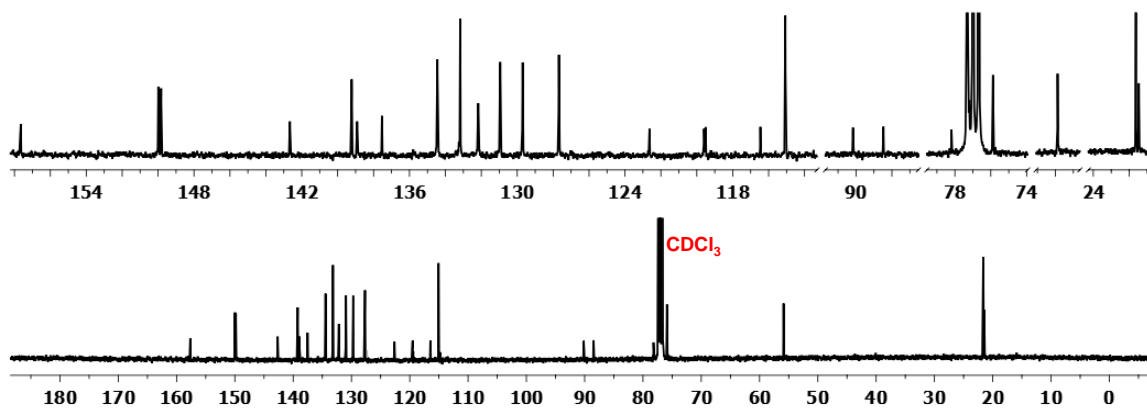


Figure S5. ^{13}C NMR of compound **3** in CDCl_3 (100 MHz, 298 K).

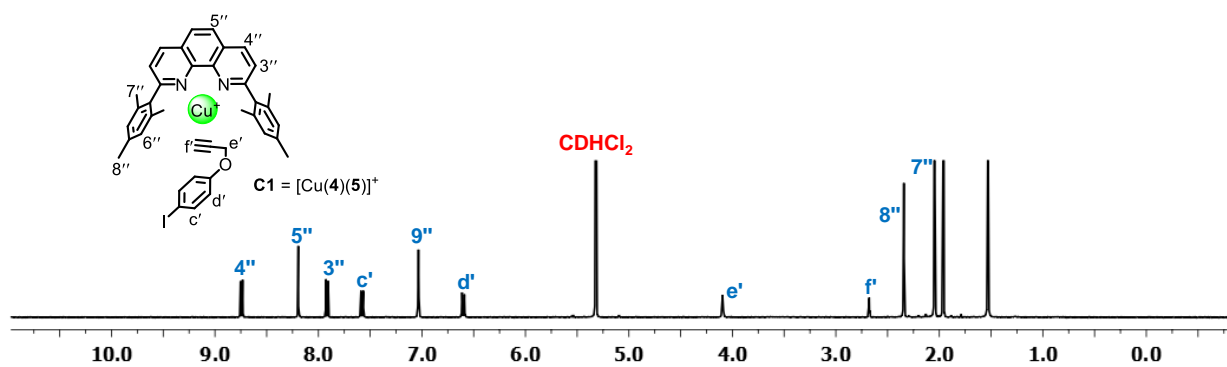


Figure S6. ^1H NMR of complex **C1** in CD_2Cl_2 (400 MHz, 298 K, 2.5 mM).

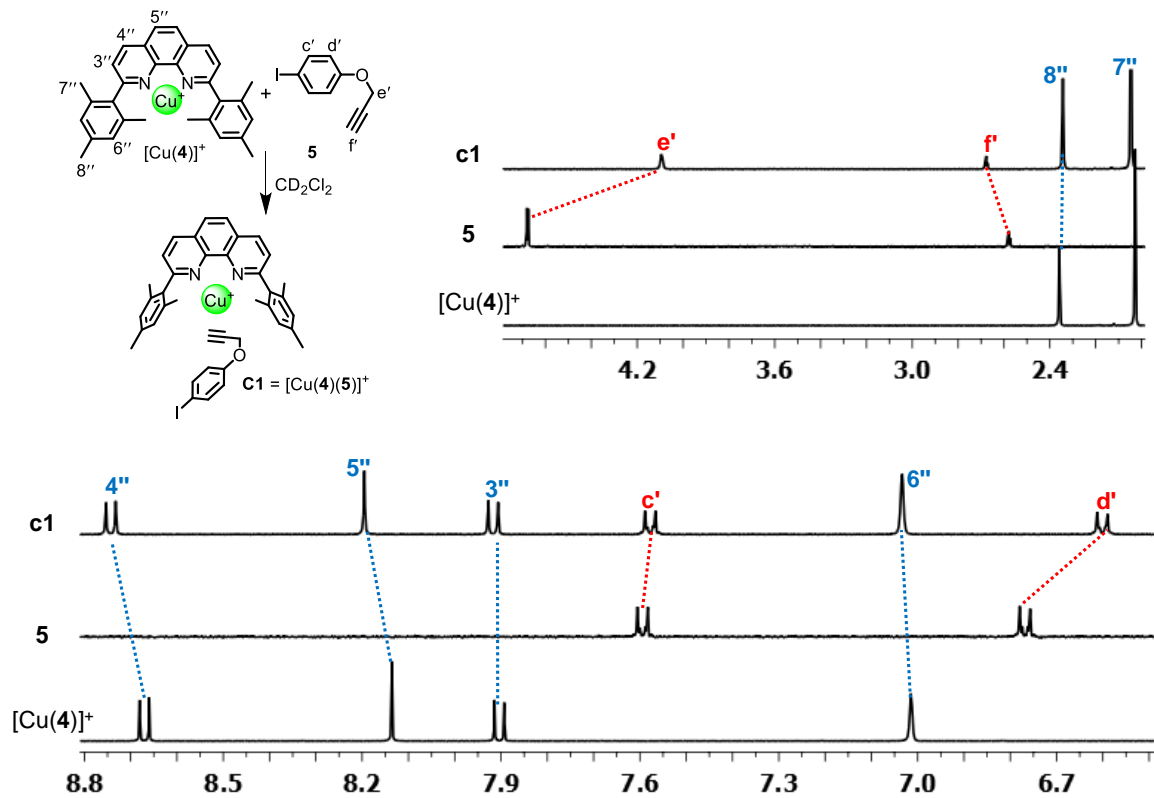


Figure S7. ^1H NMR of $[\text{Cu}(\mathbf{4})]^+$, $\mathbf{5}$ and $\mathbf{C1}$ in CD_2Cl_2 (400 MHz, 298 K, 2.5 mM).

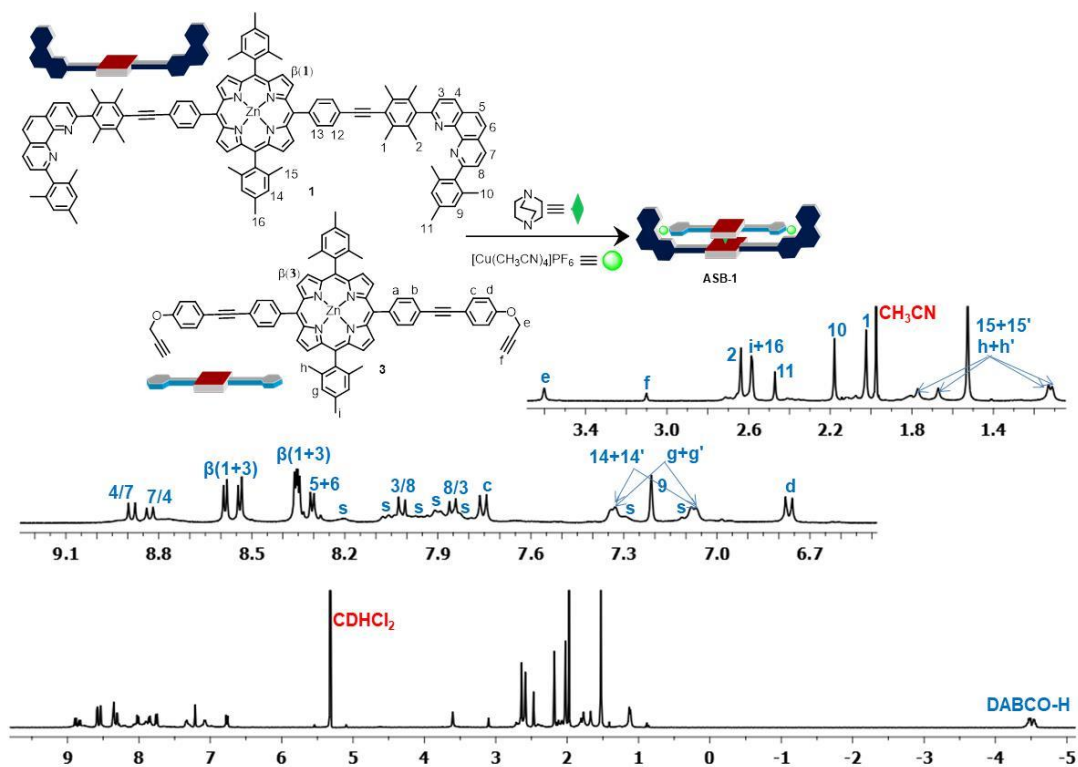


Figure S8. ^1H NMR of ASB-1 in CD_2Cl_2 (400 MHz, 298 K).

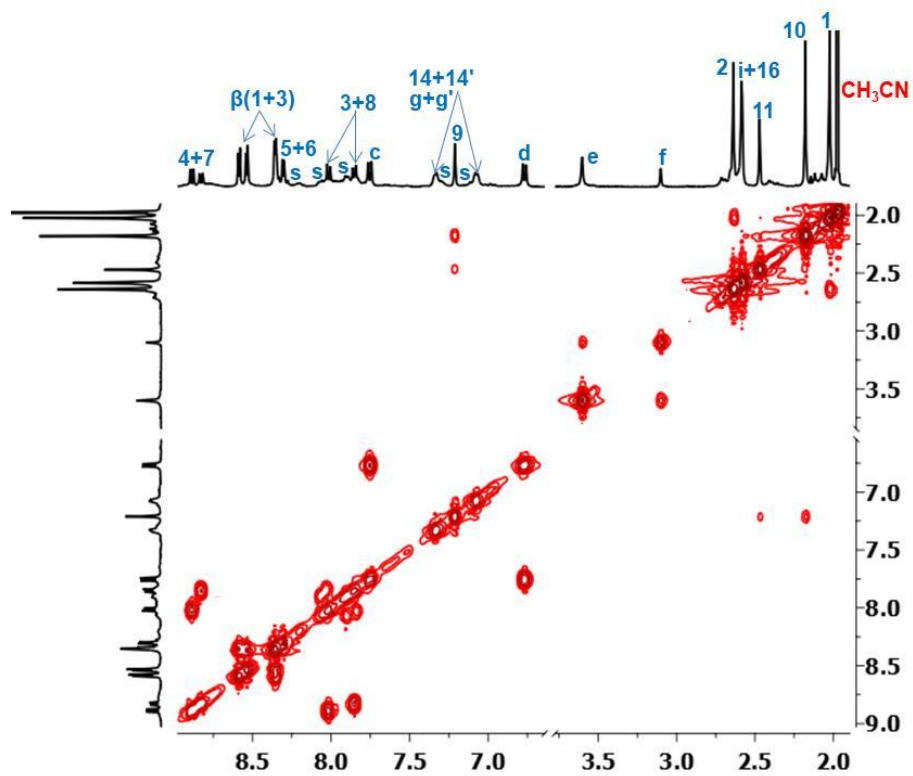


Figure S9. ^1H - ^1H COSY NMR of ASB-1 in CD_2Cl_2 (400 MHz, 298 K).

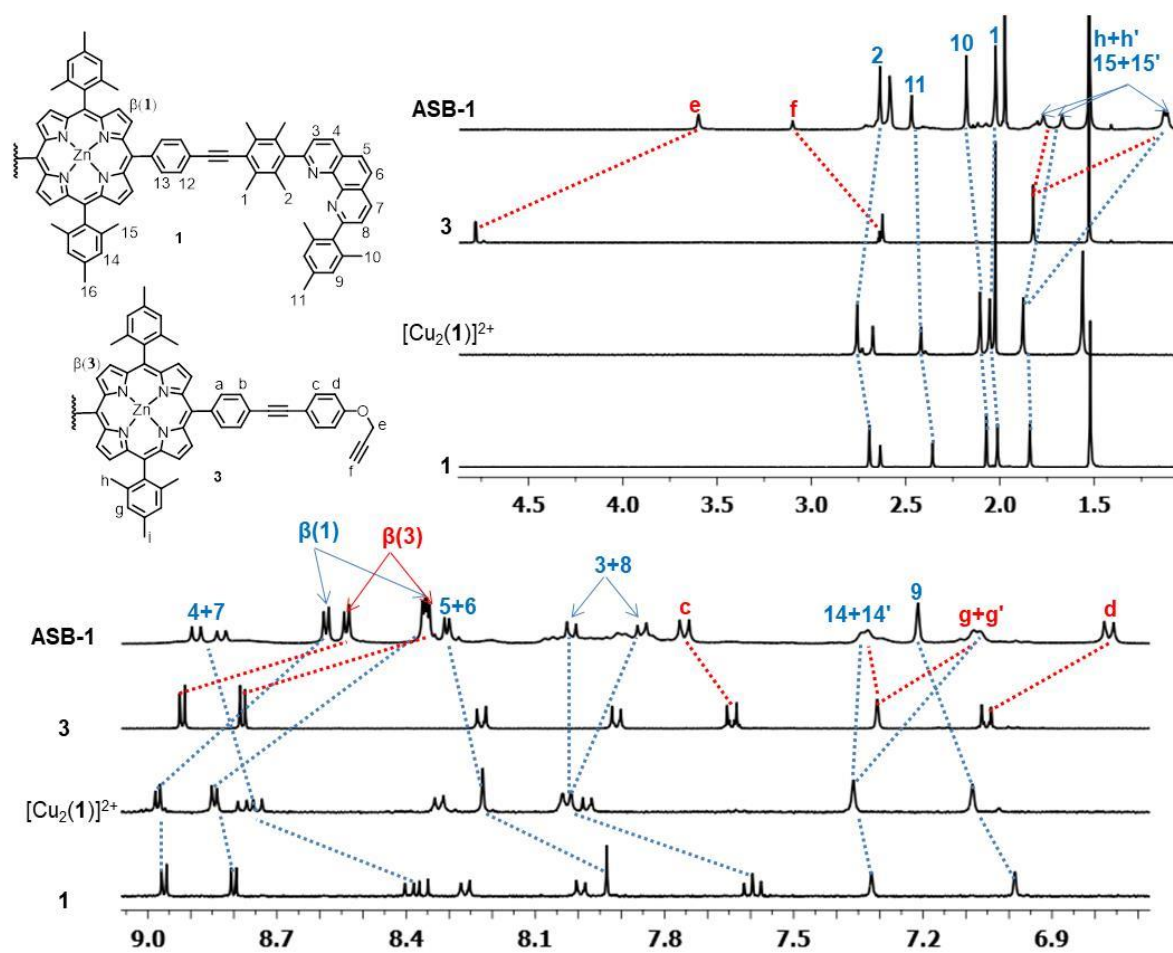


Figure S10. ^1H NMR of **1**, $[\text{Cu}_2(\mathbf{1})]^{2+}$, **3** and **ASB-1** in CD_2Cl_2 (400 MHz, 298 K).

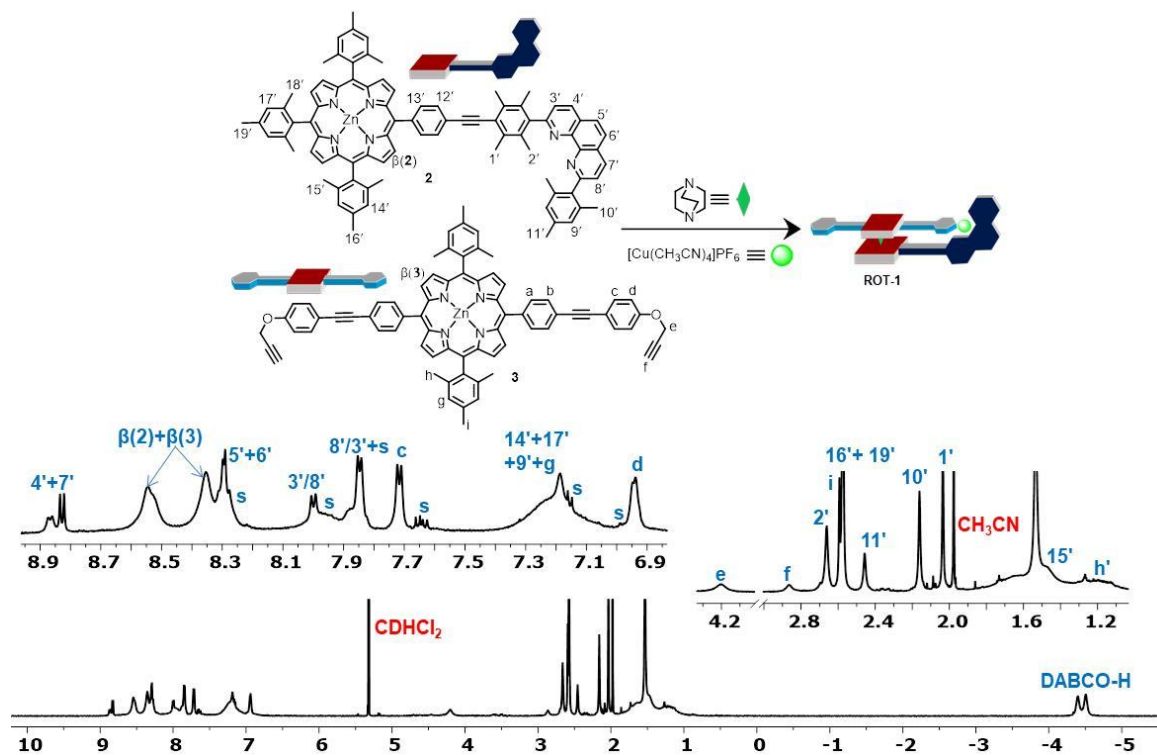


Figure S11. ^1H NMR of ROT-1 in CD_2Cl_2 (600 MHz, 298 K).

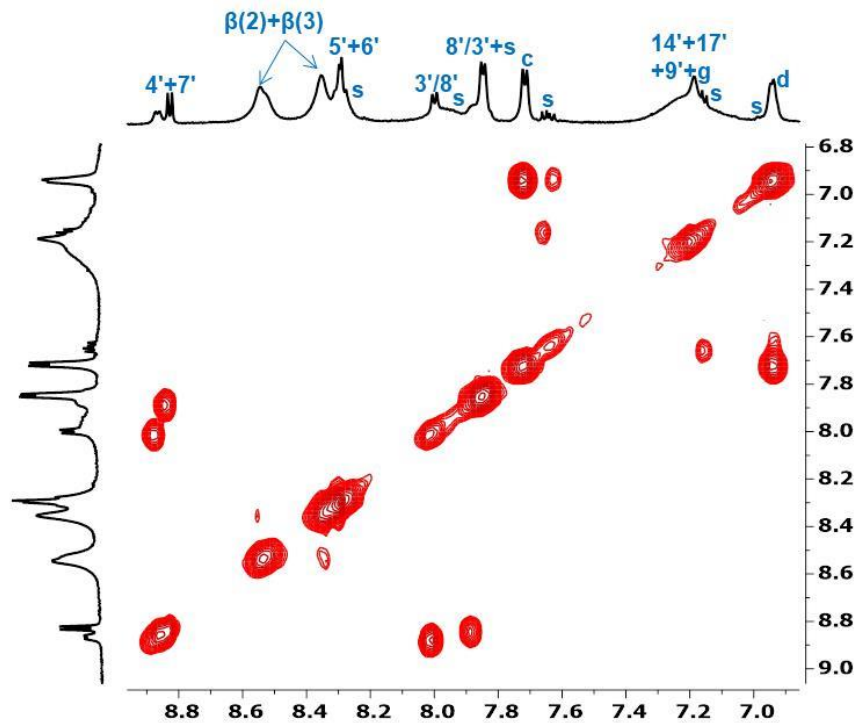


Figure S12. ^1H - ^1H COSY NMR of ROT-1 in CD_2Cl_2 (600 MHz, 298 K).

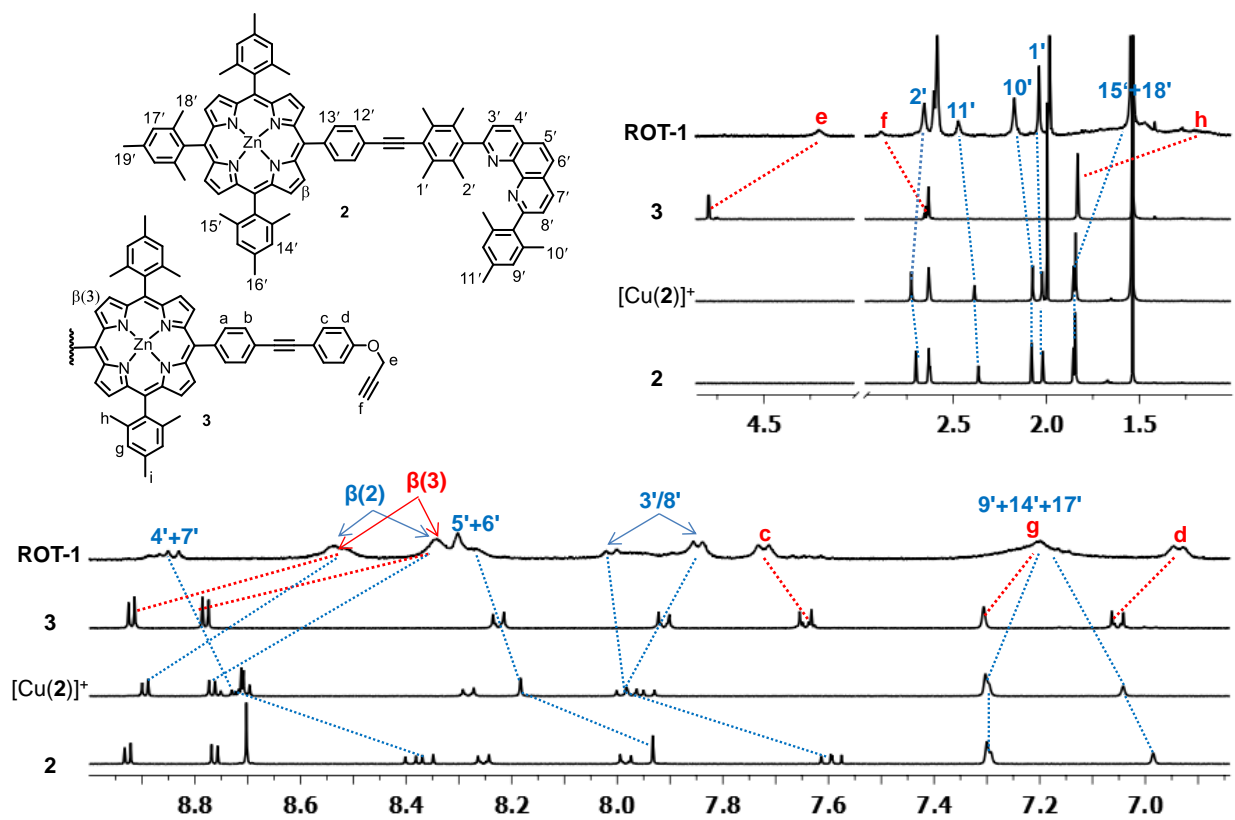


Figure S13. ^1H NMR of **2**, $[\text{Cu}(\mathbf{2})]^+$, **3** and **ROT-1** in CD_2Cl_2 (400 MHz, 298 K).

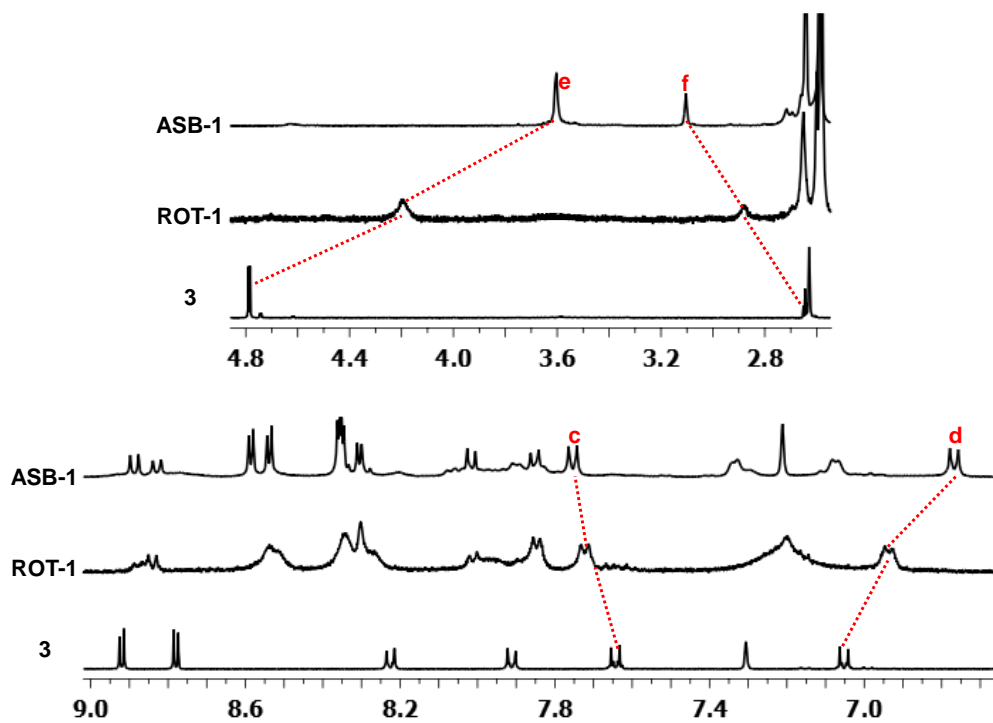


Figure S14. ¹H NMR of 3, ROT-1 and ASB-1 in CD₂Cl₂ (400 MHz, 298 K).

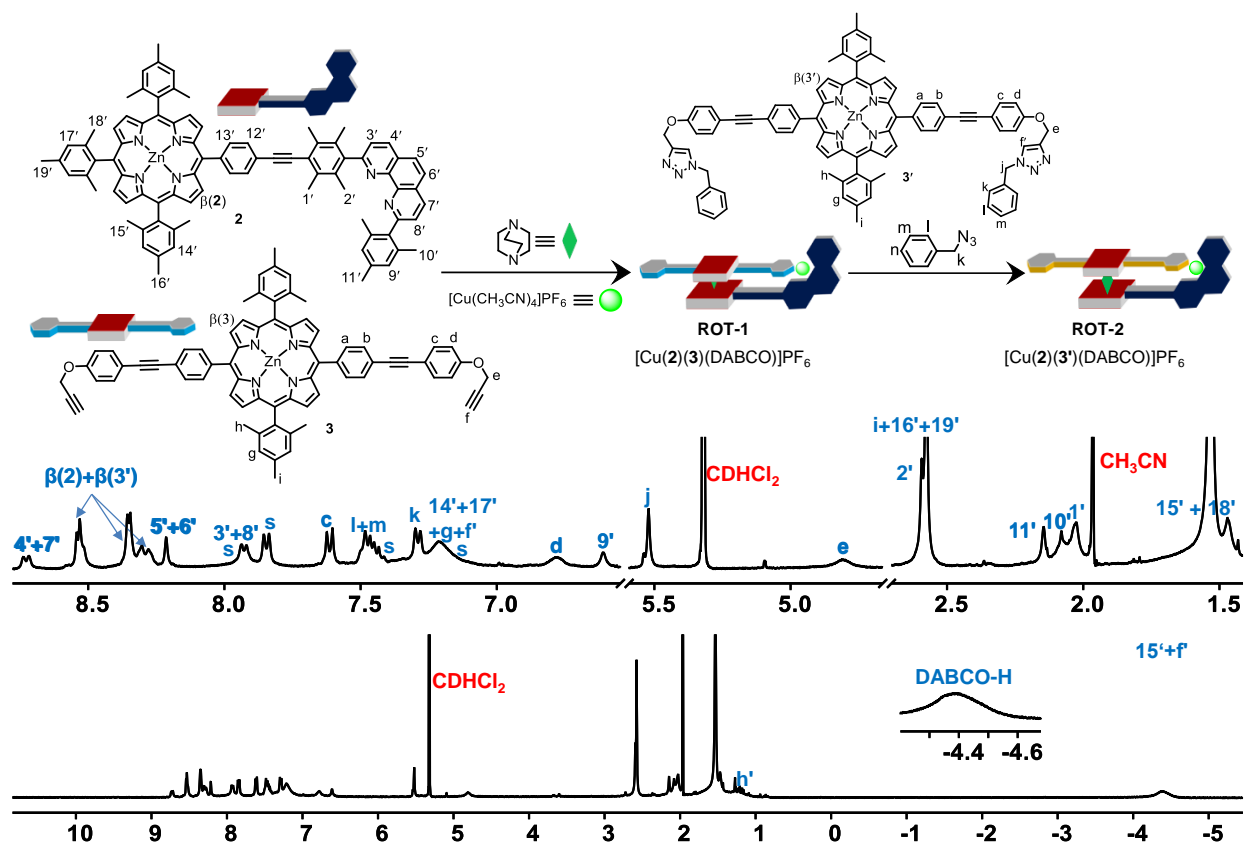


Figure S15. ^1H NMR of **ROT-2** in CD_2Cl_2 (400 MHz, 298 K).

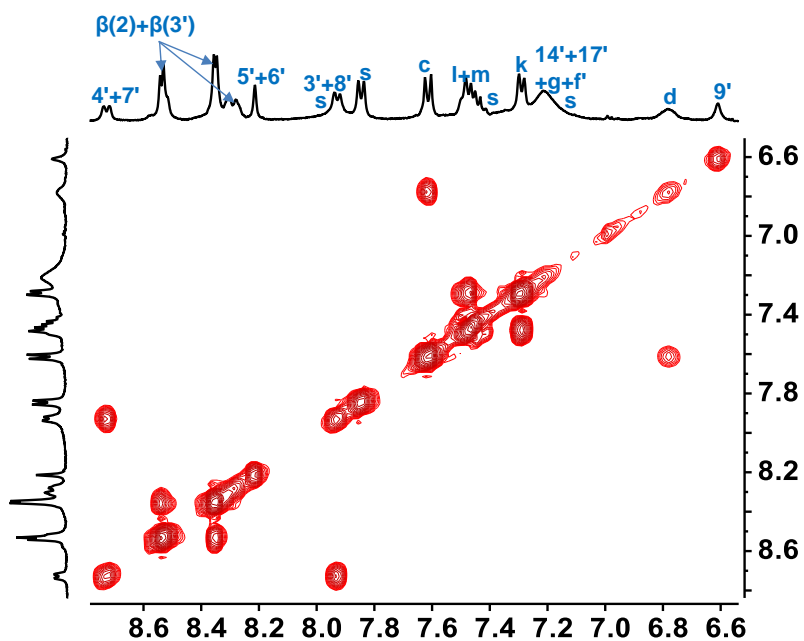


Figure S16. ^1H - ^1H COSY NMR of **ROT-2** in CD_2Cl_2 (400 MHz, 298 K).

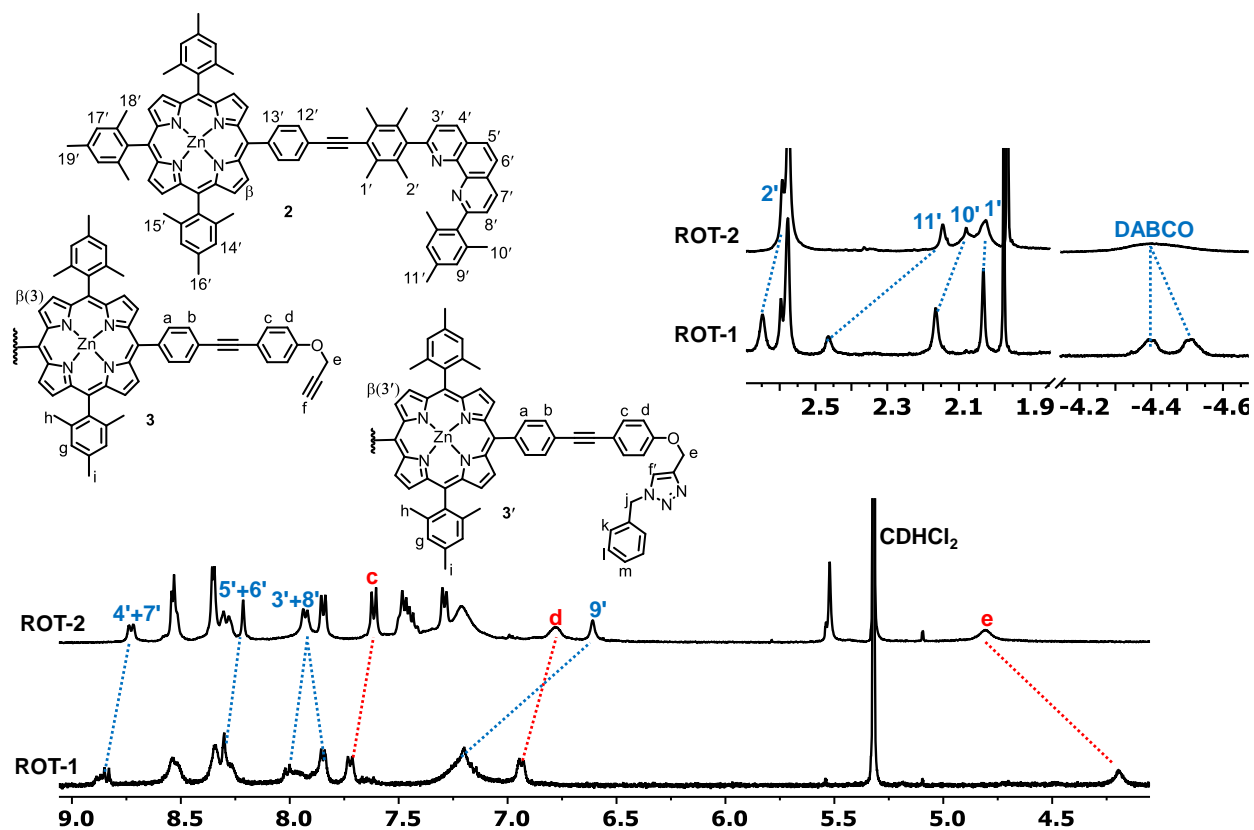


Figure S17. ^1H NMR of ROT-1 and ROT-2 in CD_2Cl_2 (400 MHz, 298 K).

3. Variable temperature ^1H NMR spectra

The kinetics of rotational exchange at various temperatures was analyzed using the program WinDNMR through simulation of the experimental ^1H NMR spectra.¹⁰ The spectra simulation was performed using the model of a 2-spin system undergoing mutual exchange and provided the rate constants. Activation parameters were determined from an Eyring plot.

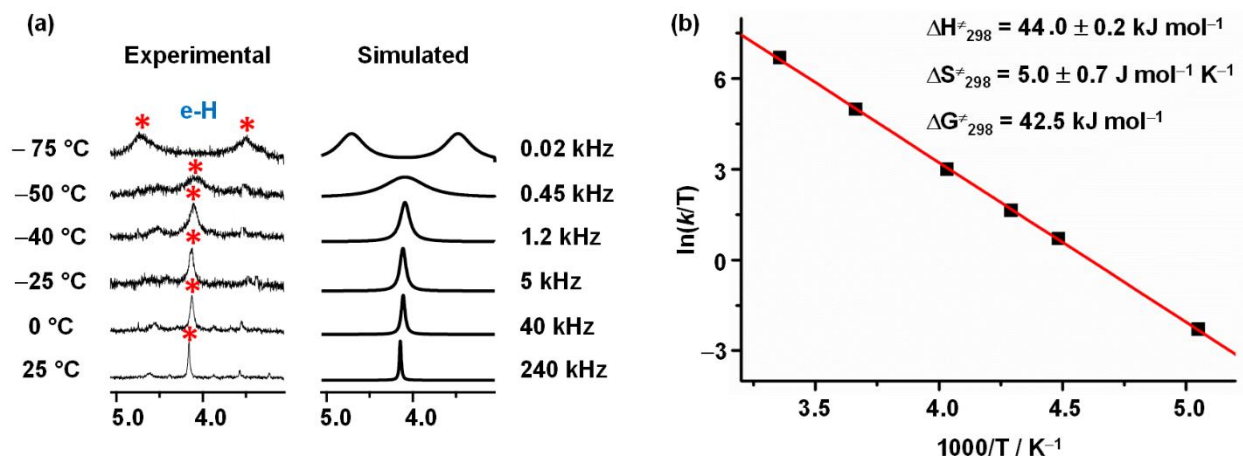


Figure S18. (a) VT ^1H -NMR (600 MHz) of **ROT-1** in CD_2Cl_2 shows the splitting of proton signal e-H in 1:1 ratio. The corresponding rate constant at different temperatures was calculated from the simulation. (b) Eyring plot for exchange frequency in nanorotor **ROT-1**.

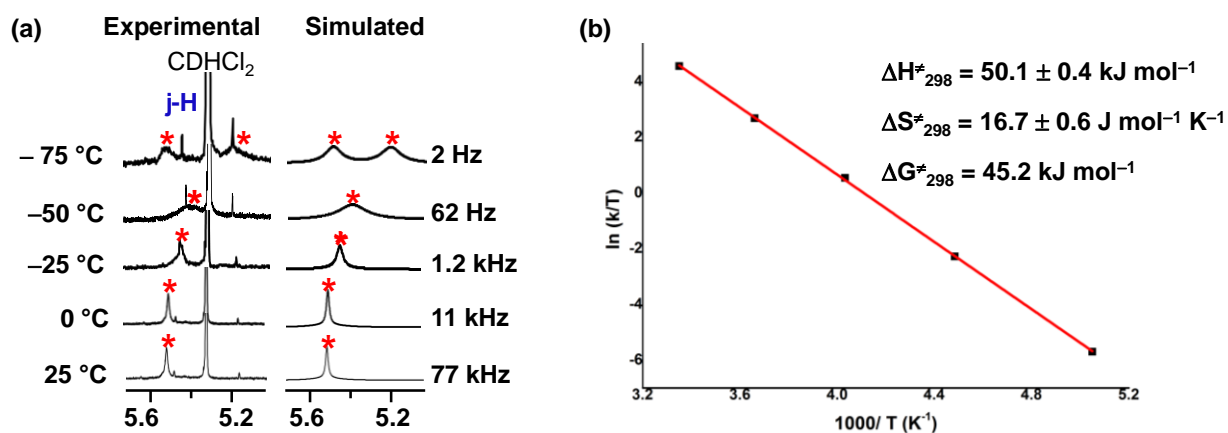


Figure S19. (a) VT ^1H -NMR (600 MHz) of **ROT-2** in CD_2Cl_2 shows the splitting of proton signal j-H in 1:1 ratio. The corresponding rate constant at different temperatures was calculated from the simulation. (b) Eyring plot for exchange frequency in nanorotor **ROT-2**.

4. DOSY NMR spectra

Calculation of hydrodynamic radius from DOSY

The diffusion coefficient D of each assembly was obtained from the DOSY spectrum, and the corresponding hydrodynamic radius was calculated by using the Stokes-Einstein equation:

$$r = k_B T / 6\pi\eta D$$

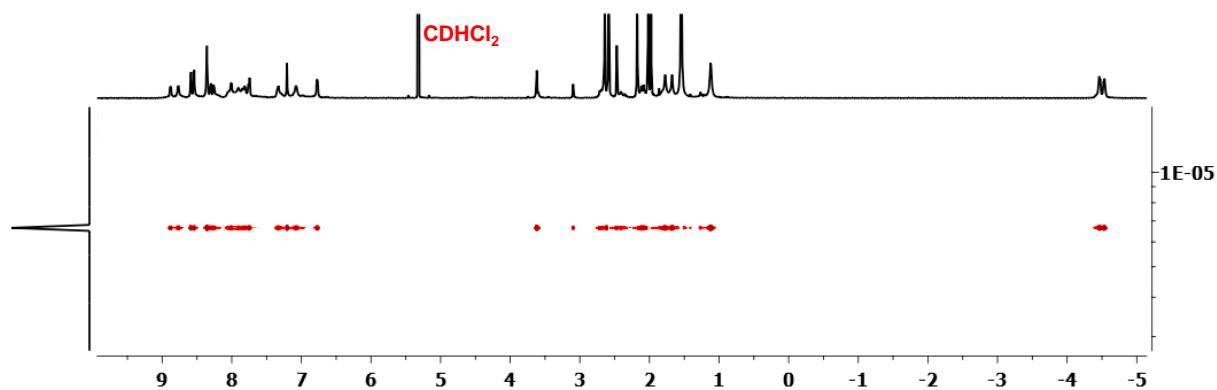


Figure S20. DOSY NMR of **ASB-1** in CD_2Cl_2 (600 MHz, 298 K). Diffusion coefficient $D = 4.8 \times 10^{-10} \text{ m}^2 \text{ s}^{-1}$, hydrodynamic radius $r = 11.4 \text{ \AA}$.

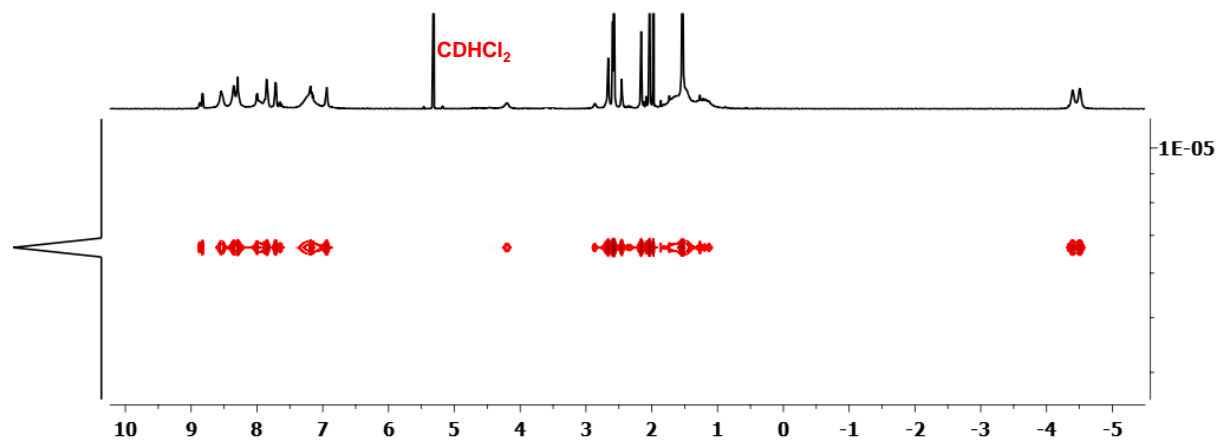


Figure S21. DOSY NMR of **ROT-1** in CD_2Cl_2 (600 MHz, 298 K). Diffusion coefficient $D = 4.8 \times 10^{-10} \text{ m}^2 \text{ s}^{-1}$, hydrodynamic radius $r = 11.4 \text{ \AA}$.

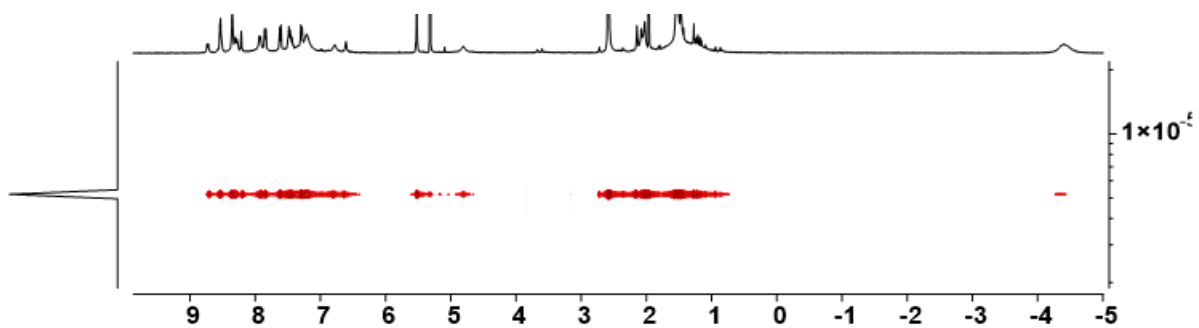


Figure S22. DOSY NMR of **ROT-2** in CD_2Cl_2 (600 MHz, 298 K). Diffusion coefficient $D = 5.0 \times 10^{-10} \text{ m}^2 \text{ s}^{-1}$, hydrodynamic radius $r = 10.9 \text{ \AA}$.

5. ESI-MS spectra

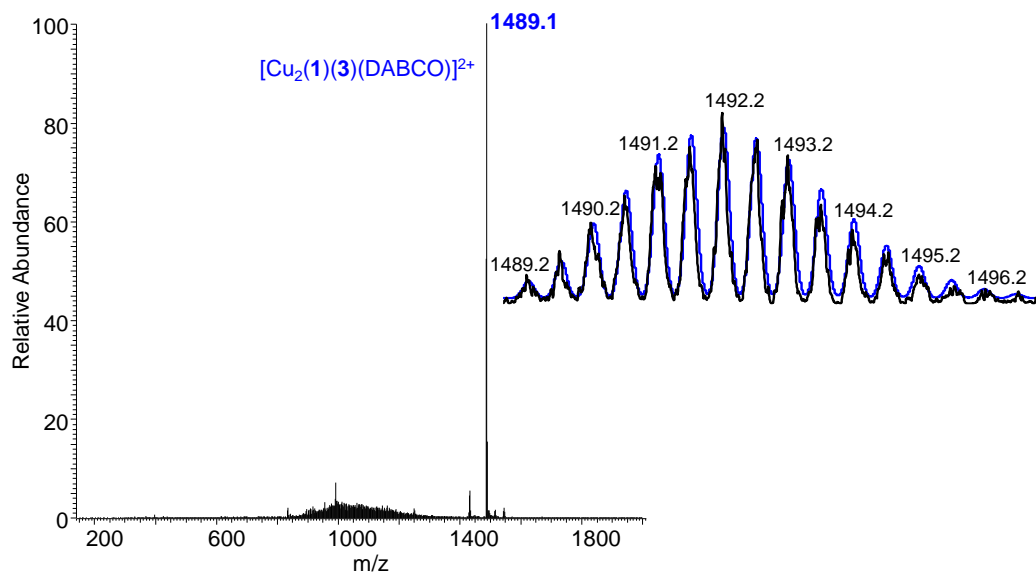


Figure S23. ESI-MS of $[\text{Cu}_2(\mathbf{1})(\mathbf{3})(\text{DABCO})]^{2+}$.

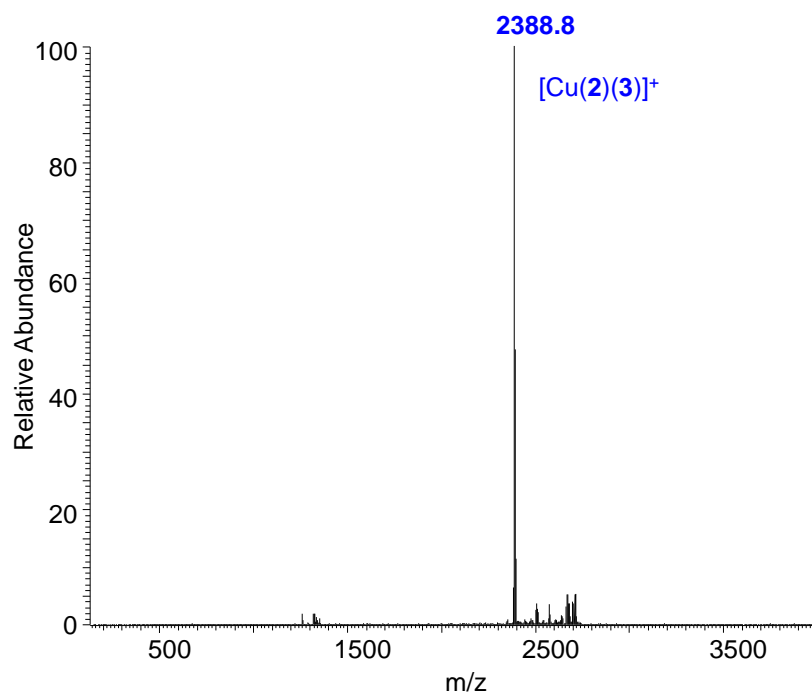


Figure S24. ESI-MS of $[\text{Cu}(\mathbf{2})(\mathbf{3})]^+$.

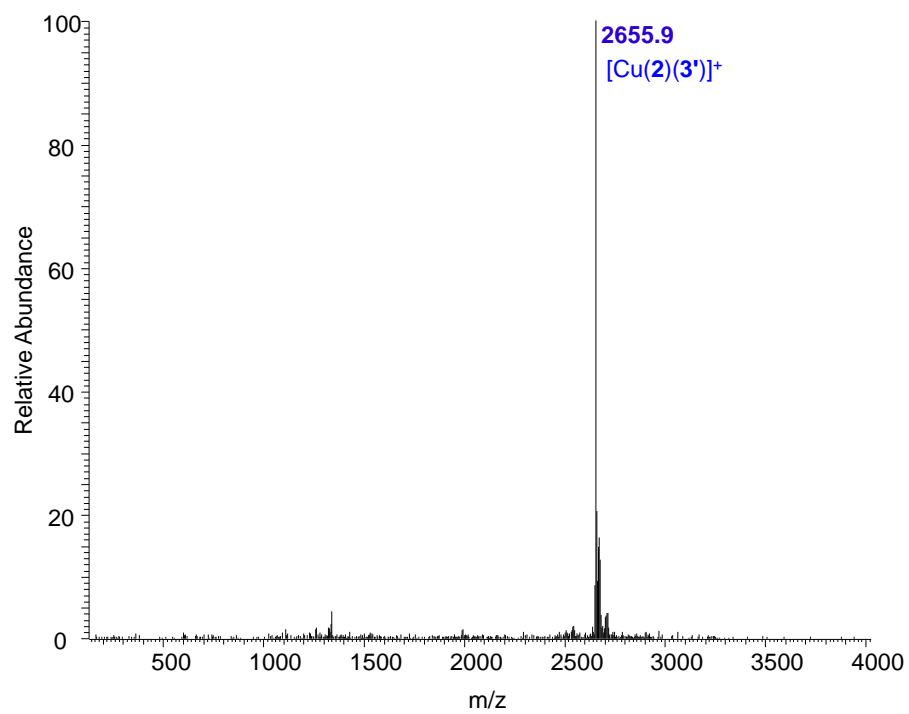


Figure S25. ESI-MS of $[\text{Cu}(\mathbf{2})(\mathbf{3}')]^+$.

6. Binding constant determination

a. Measurement of binding constant of compound **5** to [Cu(**4**)]⁺

To determine the binding constant of alkyne **5** to [Cu(**4**)]⁺, an NMR titration was performed. A 3.13 mM solution of [Cu(**4**)]⁺ was prepared in CD₂Cl₂ directly in an NMR tube. In another vial, a 62.2 mM stock solution of **5** was prepared in CDCl₃. An aliquot of 3.0 μL of **5** was added. After each addition, the ¹H NMR was recorded and the peak at 8.67 ppm (for 4''-H) was monitored for data analysis. The binding constant was determined using a nonlinear curve-fitting applying the following equation¹¹:

$$Y = Y_0 + DY * ((K * (P + x) + 1) - \sqrt{((K * (P + x) + 1)^2 - 4 * K * K * P * x)}) / (2 * K * P)$$

Y = Measured Chemical shift; Y₀ = Chemical shift of empty host solution; DY = Maximum change in chemical shift: the difference in chemical shift of a fully occupied host and an empty host; K = Binding constant; P = Total host concentration; x = Total guest concentration.

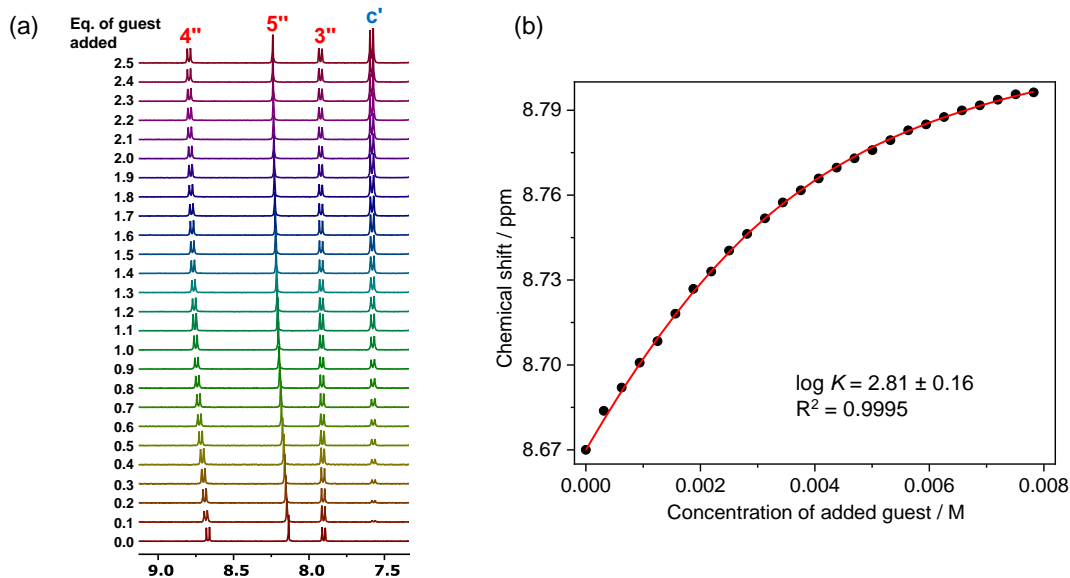
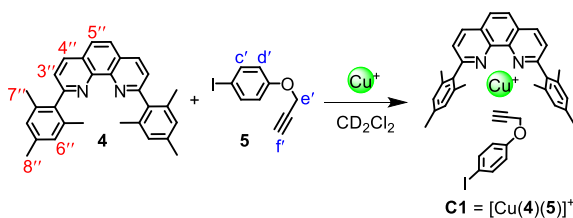


Figure S26. ¹H NMR of [Cu(**4**)]⁺ upon successive addition of compound **5** in CD₂Cl₂ (400 MHz, 298 K). (b) Curve-fitting for determination of the binding constant of **5** to [Cu(**4**)]⁺.

b. Measurement of binding constant of compound **6** to $[\text{Cu}(\mathbf{4})]^+$

To determine the binding constant of triazole **6** to $[\text{Cu}(\mathbf{4})]^+$, an NMR titration was performed. A 3.13 mM solution of $[\text{Cu}(\mathbf{4})]^+$ was prepared in CD_2Cl_2 directly in an NMR tube. In another vial, a 32.3 mM stock solution of **6** was prepared in CD_2Cl_2 . An aliquot of 4.82 μL of **6** was added. After each addition, the ^1H NMR was recorded and the peak at 7.01 ppm (for 6''-H) was monitored for data analysis. As before in chapter 6a, the binding constant was determined using non-linear curve-fitting.

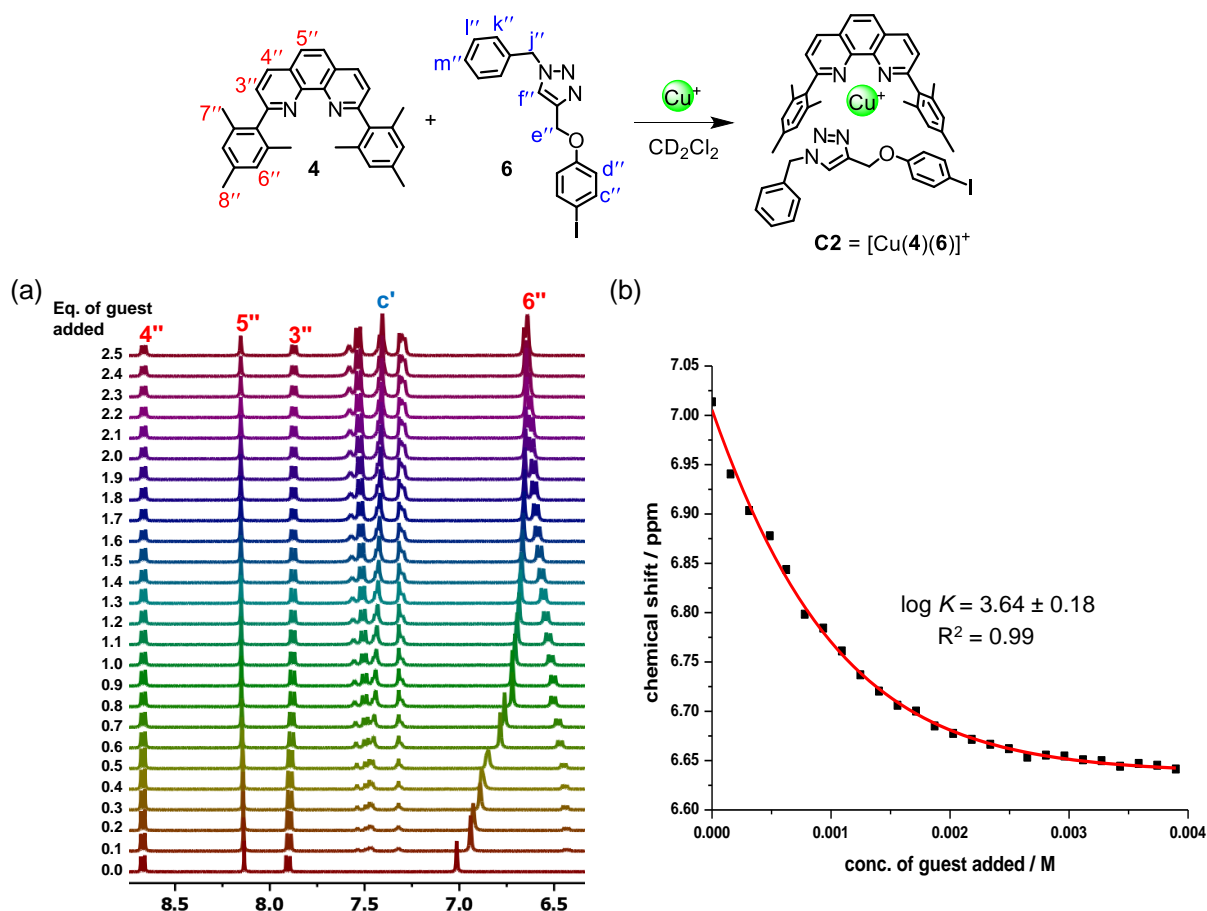


Figure S27. ^1H NMR of $[\text{Cu}(\mathbf{4})]^+$ upon successive addition of compound **6** in CD_2Cl_2 (400 MHz, 298 K). (b) Curve-fitting for determination of the binding constant of **6** to $[\text{Cu}(\mathbf{4})]^+$.

7. X-ray crystallography

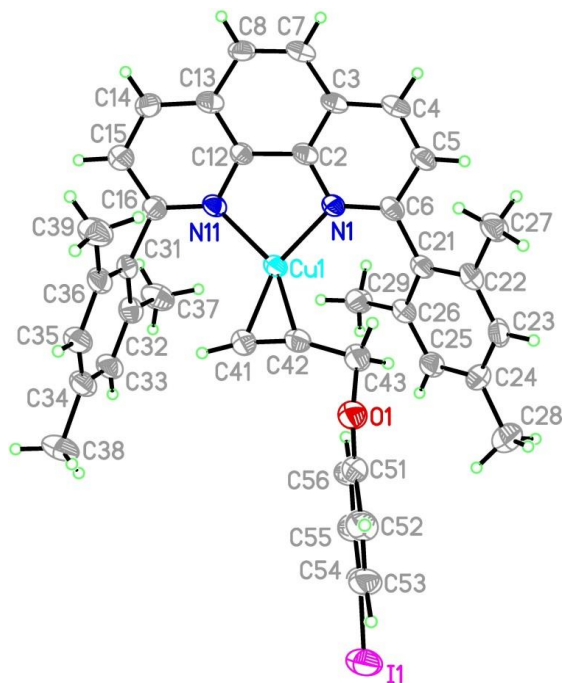


Figure S28. X-Ray crystal structure of complex **C1**. Carbon are shown in light grey; H, light green; N, blue; O, red; Cu⁺, indigo and I, violet.

Data were collected on a STOE IPDS II two-circle diffractometer with a Genix Microfocus tube with mirror optics using MoK α radiation ($\lambda = 0.71073 \text{ \AA}$). The data were scaled using the frame scaling procedure in the *X-Area* program system.¹² The structure was solved by direct methods using the program *SHELXS*¹³ and refined against F^2 with full-matrix least-squares techniques using the program *SHELXL*.¹³ The F ligands of the PF₆ anion are disordered over two positions with a site occupation factor of 0.510(17) for the major occupied orientation. The displacement ellipsoids of the disordered F atoms were restrained to an isotropic behaviour. The contribution of the unidentifiable solvent was suppressed using the *SQUEEZE* routine in *PLATON*.¹⁴ CCDC deposition number: 2199510.

Table S1. Crystal data and structure refinement for complex **C1**.

Identification code	C1
Empirical formula	C ₃₉ H ₃₅ Cu F ₆ I N ₂ O P
Formula weight	883.10
Temperature	173(2) K
Wavelength	0.71073 Å
Crystal system	Triclinic
Space group	P -1
Unit cell dimensions	a = 11.2316(6) Å a = 91.434(4)°. b = 12.5683(7) Å b = 103.968(4)°. c = 14.3333(7) Å g = 100.004(4)°.
Volume	1928.89(18) Å ³
Z	2
Density (calculated)	1.520 Mg/m ³
Absorption coefficient	1.469 mm ⁻¹
F(000)	884
Crystal size	0.120 x 0.110 x 0.020 mm ³
Theta range for data collection	3.266 to 25.027°.
Index ranges	-13<=h<=13, -14<=k<=14, -17<=l<=17
Reflections collected	29992
Independent reflections	6784 [R(int) = 0.0588]
Completeness to theta = 25.000°	99.8 %
Absorption correction	Semi-empirical from equivalents
Max. and min. transmission	1.000 and 0.609
Refinement method	Full-matrix least-squares on F ²
Data / restraints / parameters	6784 / 93 / 525
Goodness-of-fit on F ²	1.036
Final R indices [I>2sigma(I)]	R1 = 0.0549, wR2 = 0.1478
R indices (all data)	R1 = 0.0646, wR2 = 0.1594
Extinction coefficient	n/a
Largest diff. peak and hole	0.630 and -1.254 e.Å ⁻³

Table S2. Atomic coordinates ($\times 10^4$) and equivalent isotropic displacement parameters ($\text{\AA}^2 \times 10^3$) for ms3. $U(\text{eq})$ is defined as one third of the trace of the orthogonalized U_{ij} tensor.

	x	y	z	$U(\text{eq})$
I(1)	-388(1)	3709(1)	-994(1)	58(1)
Cu(1)	6284(1)	1796(1)	3159(1)	29(1)
O(1)	5252(3)	3574(3)	638(2)	40(1)
N(1)	7166(3)	2684(3)	4400(2)	27(1)
C(2)	7896(3)	2103(3)	4996(3)	29(1)
C(3)	8730(3)	2542(3)	5869(3)	30(1)
C(4)	8779(4)	3646(4)	6129(3)	34(1)
C(5)	8006(4)	4213(4)	5541(3)	34(1)
C(6)	7184(4)	3724(3)	4678(3)	28(1)
C(7)	9450(4)	1854(4)	6460(3)	35(1)
C(8)	9337(4)	796(4)	6202(3)	35(1)
N(11)	6912(3)	578(3)	3879(2)	27(1)
C(12)	7768(3)	973(3)	4716(3)	27(1)
C(13)	8478(4)	317(4)	5313(3)	32(1)
C(14)	8279(4)	-784(4)	5017(3)	36(1)
C(15)	7409(4)	-1177(4)	4173(3)	38(1)
C(16)	6729(4)	-482(3)	3612(3)	31(1)
C(21)	6280(4)	4321(3)	4083(3)	30(1)
C(22)	6700(4)	5284(3)	3683(3)	34(1)
C(23)	5824(4)	5821(3)	3137(3)	36(1)
C(24)	4544(4)	5441(4)	2972(3)	39(1)
C(25)	4146(4)	4515(4)	3393(3)	36(1)
C(26)	4983(4)	3941(3)	3957(3)	32(1)
C(27)	8078(4)	5709(4)	3802(4)	41(1)
C(28)	3611(5)	6020(5)	2335(4)	54(1)
C(29)	4486(4)	2976(4)	4433(4)	40(1)
C(31)	5764(4)	-869(3)	2702(3)	29(1)
C(32)	4498(4)	-973(3)	2698(3)	33(1)
C(33)	3601(4)	-1250(4)	1824(3)	37(1)
C(34)	3931(4)	-1432(4)	963(3)	38(1)
C(35)	5185(4)	-1338(4)	990(3)	38(1)

C(36)	6114(4)	-1065(3)	1844(3)	34(1)
C(37)	4093(5)	-769(5)	3599(4)	46(1)
C(38)	2940(5)	-1707(5)	23(4)	52(1)
C(39)	7470(4)	-931(5)	1825(4)	48(1)
C(41)	5251(5)	1412(4)	1845(3)	40(1)
C(42)	5570(4)	2391(4)	1935(3)	34(1)
C(43)	5782(5)	3518(4)	1649(3)	39(1)
C(51)	3996(4)	3587(3)	346(3)	37(1)
C(52)	3586(5)	3849(4)	-606(3)	44(1)
C(53)	2339(5)	3892(4)	-972(4)	49(1)
C(54)	1514(5)	3657(4)	-410(4)	44(1)
C(55)	1907(5)	3405(4)	532(4)	46(1)
C(56)	3155(5)	3360(4)	904(3)	45(1)
P(1)	9862(1)	2850(1)	2910(1)	50(1)
F(1)	10362(17)	3001(11)	4029(6)	103(5)
F(2)	8783(17)	3428(18)	2829(15)	158(9)
F(3)	9508(16)	2565(15)	1799(7)	74(5)
F(4)	9063(19)	1753(11)	3058(11)	144(9)
F(5)	10754(12)	3887(10)	2741(9)	77(4)
F(6)	11065(12)	2261(15)	2994(13)	121(6)
F(1')	9770(10)	3417(10)	3932(7)	75(3)
F(2')	8420(9)	2856(15)	2600(9)	98(5)
F(3')	9828(18)	2459(16)	1896(8)	100(7)
F(4')	9518(12)	1695(8)	3238(11)	100(5)
F(5')	10170(20)	4056(10)	2660(14)	149(10)
F(6')	11255(7)	2958(16)	3401(12)	148(7)

8. References

1. A. Colombo, G. D. Carlo, C. Dragonetti, M. Magni, A. O. Biroli, M. Pizzotti, D. Roberto, F. Tessore, E. Benazzi, C. A. Bignozzi, L. Casarin and S. Caramori, *Inorg. Chem.* 2017, **56**, 14189-14197
2. S. Gaikwad and M. Schmittel, *J. Org. Chem.* 2017, **82**, 343-352.
3. P. K. Biswas, S. Saha, Y. Nanaji, A. Rana and M. Schmittel, *Inorg. Chem.* 2017, **56**, 6662-6670.
4. F. Wang, Y. Zhang, Z. Liu, Z. Du, L. Zhang, J. Ren and X. Qu, *Angew. Chem. Int. Ed.* 2019, **58**, 6987–6992.
5. P. K. Biswas, S. Saha, T. Paululat and M. Schmittel, *J. Am. Chem. Soc.* 2018, **140**, 9038-9041.
6. Z. Li, D. A. Capretto, R. O. Rahaman and Chuan He, *Angew. Chem. Int. Ed.* 2007, **46**, 5184 – 5186.
7. L. F. Minuti, M. G. Memeo, S. Crespi and P. Quadrelli, *Eur. J. Org. Chem.* 2016, 821–829.
8. M. Schmittel and S. K. Samanta, *J. Org. Chem.* 2010, **75**, 5911–5919.
9. P. K. Biswas, A. Goswami, S. Saha and M. Schmittel, *Chem. Eur. J.* 2020, **26**, 14095–14099.
10. H. J. Reich, NMR Spectrum Calculations: WinDNMR, Version 7.1.13; Department of Chemistry, University of Wisconsin.
11. Y. R. Hristova, M. M. J. Smulders, J. K. Clegg, B. Breiner and J. R. Nitschke, *Chem. Sci.* 2011, **2**, 638-641.
12. Stoe & Cie, *X-AREA*. Diffractometer control program system. Stoe & Cie, Darmstadt, Germany, 2002.
13. G. M. Sheldrick, *Acta Crystallogr. Sect. A*, 2008, **64**, 112–122.
14. A. L. Spek, *Acta Crystallogr. Sect. D*, 2008, **65**, 148–155.